Ring-coupled Mach–Zehnder interferometer optimized for sensing

Matthew Terrel,* Michel J. F. Digonnet, and Shanhui Fan

Edward L. Ginzton Laboratory, Stanford University, Stanford, California 94305, USA

*Corresponding author: terrel@stanford.edu

Received 24 June 2009; revised 3 August 2009; accepted 17 August 2009;
posted 18 August 2009 (Doc. ID 113233); published 1 September 2009

We demonstrate numerically that the theoretical maximum sensitivity of a ring-coupled Mach–Zehnder interferometer (MZI) optimized as a sensor is about 30% greater than the optimized sensitivity of a conventional single-bus ring sensor with an identical ring perimeter and loss. The ring-coupled MZI sensor also achieves its greater sensitivity with a 25% lower circulating power, which is useful for the suppression of undesirable nonlinear effects. © 2009 Optical Society of America

OCIS codes: 060.2370, 060.2800, 230.5750, 280.4788.

1. Introduction

Devices based on optical microring resonators have attracted considerable attention recently, both as compact and sensitive biological and chemical sensors and for communications applications. While the majority of microring-based sensors studied so far have used either single-bus or dual-bus [1–3] configurations, devices composed of a ring side coupled to a Mach–Zehnder interferometer (MZI) have also been investigated extensively as switches [4–9] and filters [10,11] for communications applications. The root of this interest is that a ring-coupled MZI exhibits sharp Fano resonances [12], and the steep slope of these resonances can be used to produce low-power all-optical switches. Several references suggest that this same property might also be useful to produce highly sensitive sensors [8,11]. However, there has been no systematic analysis and optimization of ring-coupled MZIs as a sensor. Since the design constraints on switches, filters, and sensors are very different, a ring-coupled MZI optimized for switching is not necessarily optimized for sensing. For example, since high transmission through the ring is desirable in a switch or a filter, ring-coupled MZIs used for these applications are generally operated in the over-coupled regime [4,6,7,10], where the ring coupling ratio is much larger than the ring-waveguide loss. In contrast, a sensor based on intensity detection is optimized when it is operated at the coupling ratio and phase bias where the slope of its transmission spectrum is the steepest, which may occur in the critically coupled [2] or undercoupled [1] regimes. A recent study [13] of a device that somewhat resembles the ring-coupled MZI claimed a significant sensitivity enhancement over a single-bus ring resonator, so it is important to fully quantify the performance of the ring-coupled MZI as a sensor to determine whether it can indeed outperform conventional microring-based sensor configurations.

In this paper, we calculate the sensitivity of the ring-coupled MZI to changes in the round-trip phase in the ring as a function of all the device's parameters (coupling ratios, loss, and phase biases). This phase perturbation can be due, for example, to a change in concentration of some biological species placed against the ring waveguide [3], a change in temperature, or an applied rotation, as in the resonant fiber-optic gyroscope (RFOG) [14]. We then optimize these parameters to achieve maximum sensitivity and compare the latter to the sensitivity of an optimized conventional ring sensor. This study is quite general. In particular, it is entirely applicable to any kind of optical ring, for example microring resonators, integrated-optics rings, and fiber-based rings such

0003-6935/09/264874-06$15.00/0

as in the RFOG. We show that when properly optimized, a ring-coupled MZI allows at most a 30.5% enhancement in sensitivity over a conventional ring resonator, as well as a 25% decrease in the power circulating in the ring. The reduction in circulating power is beneficial for applications in which it is important to reduce the Kerr phase shift within the ring, for example ring-based sensors such as the RFOG, in which the Kerr phase shift causes a detrimental bias instability and thus long-term drift [14]. The overall conclusion is that the two benefits afforded by ring-coupled MZIs are welcome but the improvement over conventional configuration is not drastic. Furthermore, the introduction of an MZI adds another source of thermal instability to the sensor, which aggravates the inherent thermal instability of the ring itself. It therefore remains to be seen whether this added instability will be offset by the small improvement in sensitivity and Kerr-induced instability.

2. Ring-Coupled MZI Sensor

Figure 1(a) shows a sensor made from a ring resonator side coupled to an MZI. Narrowband light of wavelength λ is launched into one input port of the device, where it is split into the two arms of the MZI by a first coupler with a power coupling ratio κ_1. The sensing (upper) arm consists of a ring coupled to the MZI waveguide by a coupler with a power coupling ratio κ_{ring}. The round-trip phase and power attenuation in the ring are given by $\phi = 2\pi R n_{\text{eff}}/\lambda$ and $\exp(-2\pi R\alpha)$, respectively, where R is the ring radius, n_{eff} is the effective index of the mode in the ring, and α is the loss coefficient of the ring, including the coupler loss, if present. The signal phase and field transmission of the reference (lower) arm are Φ_{ref} and t_{ref}, respectively. Past the ring, the two arms are reconnected by a second coupler with coupling ratio κ_2. P_1 and P_2 are the output powers at the two output ports of this coupler. In our calculations, we assume that the loss of the waveguides that make up the MZI is negligible. We propose to use this device as a sensor by detecting the difference in the detected intensities at the two output ports $P_{\text{diff}} = P_1 - P_2$, so that its sensitivity to changes in some measurand γ is $S = dP_{\text{diff}}/d\gamma$. Using P_{diff} gives a better sensitivity than using either P_1 or P_2 because P_1 and P_2 change in response to a change in measurand typically with opposite signs, so P_{diff} typically changes faster than either P_1 or P_2.

Our goal is to maximize the sensitivity of the sensor of Fig. 1(a) to any effect that changes the round-trip phase in the ring ϕ (e.g., changes in temperature or rotation) and to see whether this sensitivity exceeds the maximum sensitivity of the single-bus ring of Fig 1(b). We write the sensitivity of the ring-coupled MZI to a measurand γ as $S = S_1 \cdot S_2$, where $S_1 = dP_{\text{diff}}/d\phi$ is the sensitivity to changes in the round-trip phase ϕ and $S_2 = d\phi/d\gamma$ is the rate of change of ϕ with respect to the measurand γ. We know how a measurand affects the phase of the signal traveling through a ring for a wide range of measurands. For biochemical sensors, the interaction of the waveguide mode's evanescent field with a dissolved analyte changes the effective index n_{eff} of the waveguide mode, thus changing ϕ [3]. If the measurand is a rotation Ω, then $S_2 = d\phi/d\Omega$ is a constant determined by the ring radius R and the wavelength [14]. If the measurand is temperature T, then $S_2 = d\phi/dT$ is determined mostly by the waveguide's thermal expansion coefficient (a change in temperature results in a change in the ring's perimeter, and thus a change in phase) and thermo-optic coefficient dn_{eff}/dT. Thus, by optimizing S_1, we optimize the device's sensitivity to any measurand that perturbs ϕ. To find the optimum sensitivity to any given measurand, we simply multiply the optimum value of S_1 by the proper value of S_2.

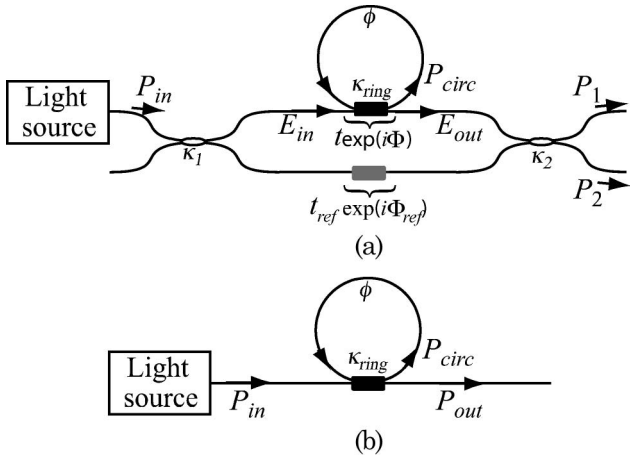

Fig. 1. (a) Ring side-coupled to a MZI.(b) Single-bus ring.

3. General Optimization of the Mach–Zehnder Interferometer

For simplicity, and to broaden the applicability of our results, we first consider the more general case of an MZI with sensing-arm transmitted amplitude and phase $t(\phi)$ and $\Phi(\phi)$ that are arbitrary functions of ϕ. For a given pair of functions $t(\phi)$ and $\Phi(\phi)$, we need to choose the four parameters in the MZI (namely κ_1, κ_2, t_{ref}, and Φ_{ref}) so as to maximize S_1. Once we have found the optimum MZI parameters for the arbitrary functions $t(\phi)$ and $\Phi(\phi)$, it is straightforward to optimize the ring-coupled MZI by substituting the ring's transmitted amplitude and phase for $t(\phi)$ and $\Phi(\phi)$.

One should reasonably expect that maximum sensitivity should occur when $t_{\text{ref}} = 1$, otherwise the MZI is simply wasting some of the power in the reference arm. Thus, only three parameters need to be optimized, namely the two coupling coefficients κ_1 and κ_2 and the bias phase Φ_{ref}. To do so, we started with the published equations for the dependence of P_1 and P_2 on κ_1, κ_2, t_{ref}, Φ_{ref}, $t(\phi)$, and $\Phi(\phi)$ [11]. To find S_1, we calculated the derivative of $P_{\text{diff}} = P_1 - P_2$ with respect to ϕ, taking into account the fact that

$t(\phi)$ and $\Phi(\phi)$ are functions of ϕ. For $t_{\mathrm{ref}} = 1$, the sensitivity comes out to be

$$S_1/P_{\mathrm{in}} = -[4A\cos(\Phi_{\mathrm{ref}} - \Phi(\phi)) + 2Bt(\phi)]t'(\phi) - 4A\sin(\Phi_{\mathrm{ref}} - \Phi(\phi))t(\phi)\Phi'(\phi),$$
$$A = \sqrt{\kappa_1\kappa_2(1-\kappa_1)(1-\kappa_2)},$$
$$B = \kappa_1 + 2\kappa_2 - 2\kappa_1\kappa_2 - 1. \quad (1)$$

Here, $t'(\phi)$ and $\Phi'(\phi)$ are the derivatives of $t(\phi)$ and $\Phi(\phi)$ with respect to ϕ, respectively. Straightforward manipulation of Eq. (1) shows that S_1 has extrema when κ_1, κ_2, and Φ_{ref} take the values

$$\Phi_{\mathrm{ref}} = \Phi + \tan^{-1}\left(\frac{t\Phi'}{t'}\right) + m\pi,$$
$$\kappa_1 = \frac{t'^2 - 2t'^2t^2 + t^2\Phi'^2}{2t'^2 - 2t'^2t^2 + 2t^2\Phi'^2},$$
$$\kappa_2 = \frac{(1-t^2)t'^2 + t^2\Phi'^2 \pm t't\sqrt{t'^2 + t^2(\Phi'^2 - t'^2)}}{2(1-t^2)t'^2 + 2t^2\Phi'^2}, \quad (2)$$

where m is either 0 or 1 and t, t', Φ, and Φ' denote $t(\phi)$, $t'(\phi)$, $\Phi(\phi)$, and $\Phi'(\phi)$, respectively. Equation (2) states that there are two possible solutions for both Φ_{ref} and κ_2. Consequently, there are four combinations of the parameters κ_1, κ_2, and Φ_{ref} that produce an optimum in the sensitivity of an MZI.

In the simpler limiting case when variations in ϕ affect only the phase of the signal in the sensing arm, but not the amplitude [i.e., $t'(\phi) = 0$ and $\Phi'(\phi) \neq 0$], these equations show that the MZI is optimum for $\kappa_1 = \kappa_2 = 0.5$ and $\Phi_{\mathrm{ref}} - \Phi(\phi) = \pm\pi/2$. However, in the more general case when variations in ϕ affect both the phase and the amplitude of the signal in the sensing arm [i.e., $t'(\phi) \neq 0$ and $\Phi'(\phi) \neq 0$], the solution is not so simple. In order to find the absolute optimum configuration in this case, we compared the sensitivity of the four solutions and identified the combination that yields the highest sensitivity. [Note that for some combination of parameters $t(\phi)$ and $\Phi(\phi)$, the solution for κ_1 and/or one or both of the solutions for κ_2 is less than 0 or larger than 1, i.e., they are unphysical mathematical solutions. In such cases, we used 0 or 1 as the solution, whichever is closest.]

4. Optimized Ring-Coupled Mach–Zehnder Interferometer

To obtain the optimum sensitivity of a ring-coupled MZI all we need to do is insert the transmission amplitude $t(\phi)$ and phase $\Phi(\phi)$ of a ring resonator in Eq. (2) to obtain the optimum values of the MZI parameters (κ_1, κ_2, and Φ_{ref}), then insert these values in Eq. (1) to obtain the maximum sensitivity. For a single ring, $t(\phi)$ and $\Phi(\phi)$ can be calculated from the known transmission function of a ring [8]:

$$\frac{E_{\mathrm{out}}}{E_{\mathrm{in}}} = \frac{e^{i\phi - \pi R\alpha} - \sqrt{1-\kappa_{\mathrm{ring}}}}{e^{i\phi - \pi R\alpha}\sqrt{1-\kappa_{\mathrm{ring}}} - 1}, \quad (3)$$

where E_{in} is the electric field at the input of the ring, E_{out} is the field at the output of the ring [see Fig. 1(a)], and ϕ is the phase shift experienced by the signal as it travels once around the ring. The amplitude $t(\phi)$ and phase $\Phi(\phi)$ are therefore given by $t = |E_{\mathrm{out}}|$ and $\Phi = \arg(E_{\mathrm{out}})$, respectively. We have ignored the phase due to the waveguide that makes up the upper arm of the MZI, which simply adds a constant offset to the phase due to the ring.

We note that in general, whenever the sensitivity of the ring-coupled MZI is significant, $\pi R\alpha$, κ_{ring} and ϕ (modulo 2π) are all much smaller than 1. Physically, this corresponds to a high-finesse ring with a small detuning from resonance. In this case, $\exp(-\pi R\alpha) \approx 1 - \pi R\alpha$, $(1-\kappa_{\mathrm{ring}})^{1/2} \approx 1 - \kappa_{\mathrm{ring}}/2$, and $\exp(i\phi) \approx 1 + i\phi$. Using these approximations, the exact expression for the transmitted field given in Eq. (3) is well approximated by

$$\frac{E_{\mathrm{out}}}{E_{\mathrm{in}}} \approx \frac{1 - \kappa_{\mathrm{norm}} - 2i\phi_{\mathrm{norm}}}{1 + \kappa_{\mathrm{norm}} - 2i\phi_{\mathrm{norm}}}, \quad (4)$$

where $\kappa_{\mathrm{norm}} = \kappa_{\mathrm{ring}}/2\pi R\alpha = \kappa_{\mathrm{ring}}/\kappa_c$ is the normalized coupling ratio and $\phi_{\mathrm{norm}} = \phi/2\pi R\alpha$ is the normalized round-trip phase. Equation (4) shows that the ring's transmission depends only on the normalized values of the round-trip phase and coupling. Hence, κ_{norm} and ϕ_{norm} completely determine the normalized sensitivity $S_{1,\mathrm{norm}} = (1/P_{\mathrm{in}})dP_{\mathrm{diff}}/d\phi_{\mathrm{norm}} = 2\pi R\alpha S_1/P_{\mathrm{in}}$. We also calculated the power circulating in the ring, P_{circ} (see Fig. 1), using this same approximation. It is straightforward to show that under this approximation the normalized circulating power $P_{\mathrm{circ,norm}} = 2\pi R\alpha\ P_{\mathrm{circ}}/P_{\mathrm{in}}$ is also completely determined by κ_{norm} and ϕ_{norm}. While the sensitivity S_1 and circulating power P_{circ} in any particular ring-coupled MZI depend on the input power and the ring's coupling, round-trip phase, and round-trip loss, the normalized sensitivity $S_{1,\mathrm{norm}}$ and circulating power $P_{\mathrm{circ,norm}}$ depend only on the normalized coupling and phase. Thus, when operated at the same values of κ_{norm} and ϕ_{norm}, $S_{1,\mathrm{norm}}$ and $P_{\mathrm{circ,norm}}$ are the same for all high-finesse ring-coupled MZI sensors, regardless of the round-trip loss.

In order to find the maximum sensitivity of the ring-coupled MZI, we must find the optimum values for the bias ring round-trip phase ϕ and the coupling κ_{ring}. Although it is possible to obtain an analytical expression for S_1 as a function of ϕ and κ_{ring} from Eqs. (1)–(3), this expression is cumbersome enough that attempting to optimize S_1 analytically with respect to ϕ and κ_{ring} leads to unwieldy expressions. As an alternative, we resorted to numerical evaluation of Eqs. (1)–(3). For a given set of ring parameters R and α we systematically sampled κ_{ring} and ϕ over a wide range of values. For every (κ_{ring}, ϕ) pair, we numerically calculated $t(\phi)$, $\Phi(\phi)$, $t'(\phi)$, and $\Phi'(\phi)$ using the exact formula for the ring's transmission [Eq. (3)]. Then, we calculated the values of the MZI parameters that optimize the sensitivity using Eq. (2) and this maximum ensitivity using Eq. (1). We

then repeated this process for another (κ_{ring}, ϕ) pair, until we found the optimum phase bias and sensitivity for each value of κ_{ring}, as well as the (κ_{ring}, ϕ) pair that gave the absolute highest sensitivity.

In the following numerical analysis, we used the method described above, with $R = 5\,\text{cm}$ and a ring loss of $0.2\,\text{dB/km}$ to simulate a ring made from a low-loss single-mode silica fiber operated at a wavelength around $\lambda = 1.5\,\mu\text{m}$. We searched for optimum performance for values of ϕ ranging from -0.002 to $0.002\,\text{rad}$, which fully cover the ring's resonance [see Fig. 3(a)]. We used values of κ_{ring} ranging from $0.1\kappa_c$ to $20\kappa_c$, where $\kappa_c = 2\pi R\alpha$ is the critical coupling. This range was chosen because it covers the undercoupled, critically coupled, and overcoupled cases, allowing us to evaluate how the ring-coupled MZI performs in each of these regimes. The single-bus ring was optimized by using this same method with the same fixed values of R and α, while keeping $\kappa_1 = \kappa_2 = 0$.

Figure 2 shows the calculated normalized sensitivity $S_{1,\text{norm}}$ of an optimally phase biased ring-coupled MZI as a function of $\kappa_{\text{norm}} = \kappa_{\text{ring}}/\kappa_c$, as well as the sensitivity of a properly biased single-bus ring, both optimized according to the process described above. In agreement with previous work [1], we find that the sensitivity of the single-bus ring is maximum at half critical coupling. Unlike the single-bus ring, the ring-coupled MZI reaches its maximum sensitivity at critical coupling. This maximum sensitivity is 30.5% greater than that of an optimized single-bus ring with the same input power. At critical coupling, the optimum MZI parameters are $\kappa_1 = \kappa_2 = 0.5$ and $\Phi_{\text{ref}} = \pi/2$. While the sensitivity of the optimized ring-coupled MZI decreases as the coupling is increased beyond critical coupling, it decreases much more slowly than the sensitivity of the single-bus ring (see Fig. 2). This figure also shows the normalized circulating power $P_{\text{circ,norm}}$ in the ring for the optimized ring-coupled MZI as a function of κ_{norm} and the same quantity for the optimally phase-biased single ring. We note that when the sensitivity of the ring-coupled MZI is maximized, the power circulating in the ring is 25% lower than the power circulating in the optimized single-bus ring (i.e., at half-critical coupling). This is because in the optimized ring-coupled MZI, (1) only half of the total power from the source is incident on the ring (the other half is sent into the reference arm), and (2) the ring-coupled MZI is optimized at critical coupling (whereas the single-bus ring is optimized at half-critical coupling, i.e., for lower circulating power). A second benefit of the ring-coupled MZI sensor is therefore that it provides a greater sensitivity with a lower circulating power. In some applications where a high circulating power is undesirable because it induces a deleterious Kerr phase shift, such as an RFOG, this reduction in circulating power may be more useful than the increased sensitivity. In this case, the input power in the ring-coupled MZI can be reduced by a factor of 1.305 while still retaining the same sensitivity, resulting in a device with a sensitivity equal to that of the optimized single-bus ring but with $1.305/0.75 \approx 1.74$ times less Kerr-induced phase drift.

While Fig. 2 was generated using the exact expressions for the ring's transmission [Eq. (3)] and circulating power for particular numerical values of R and α, the above analysis of Eq. (4) shows that if the finesse is sufficiently large the normalized sensitivity and circulating power do not depend on the particular value chosen for the round-trip attenuation. We verified the validity of this approximation by recalculating the normalized sensitivity and circulating power using the approximate equation [Eq. (4)] for the ring's transmission and comparing the results given by this high-finesse approximation to the exact results for several different values of the round-trip loss. For $R = 5\,\text{cm}$ and a ring loss of $0.2\,\text{dB/km}$ ($2\pi R\alpha = 1.45 \times 10^{-5}$), as used to generate Fig. 2, the agreement between the two methods is excellent, with less than 1% error across the entire range of κ_{norm} values shown in Fig. 2. Even in the much higher loss case when $2\pi R\alpha = 0.01$, the approximate method predicts sensitivity values that are within 10% of the exact values across the range of κ_{norm} values considered in Fig. 2. Thus, the normalized results plotted in Fig. 2 are valid for all high-finesse ring-coupled MZI sensors, regardless of the particular round-trip loss value.

To get a better sense for the behavior of this system at critical coupling, we show in Fig. 3(a) the output powers P_1 and P_2 as a function of the ring round-trip phase (modulo 2π) for the optimum ring-coupled MZI system ($\kappa_1 = \kappa_2 = 0.5$, $\Phi_{\text{ref}} = \pi/2$, $\kappa_{\text{norm}} = 1$), with $\alpha = 0.2\,\text{dB/km}$ and $R = 5\,\text{cm}$. As is characteristic of systems exhibiting a Fano resonance, both P_1 and P_2 are asymmetric with respect to the resonance at $\phi = 0$. Figure 3(b) shows the sensitivity, which is maximized on resonance. At the optimum bias point ($\phi = 0$), both P_1 and P_2 are equal to $P_{\text{in}}/4$, and the slopes of P_1 and P_2 are equal in magnitude but

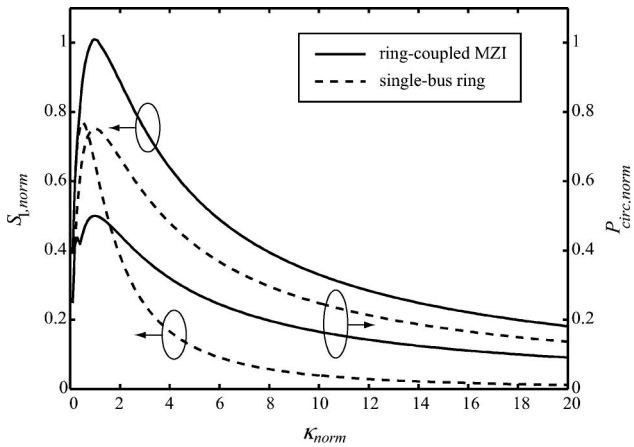

Fig. 2. Calculated normalized sensitivity and circulating power in a ring resonator and a ring-coupled MZI as a function of the normalized ring coupling ratio.

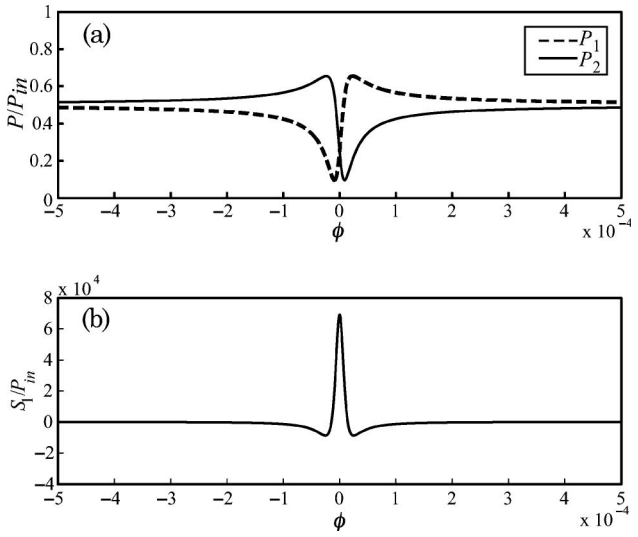

Fig. 3. (a) P_1, and P_2 of the optimized ring-coupled MZI as ϕ is varied. (b) Sensitivity of the ring-coupled MZI as ϕ is varied.

opposite in sign so that the slope of P_{diff} (i.e., the sensitivity) is twice the slope of P_1. In this optimized sensor neither P_1 nor P_2 has a large contrast ratio, as would be the case in a ring-coupled MZI optimized as a switch. Additionally, near the resonance, a significant fraction of the input power is lost to propagation loss in the ring, since the ring is operated at critical coupling. This is also qualitatively unlike the behavior of an optimized switch, which ideally has very little loss.

One conclusion from this study is that the sensitivity enhancement offered by the asymmetric Fano resonances of the ring-coupled MZI is greatly diminished when the loss is comparable to the coupling. When the ring is strongly overcoupled (i.e., $\kappa_{\text{norm}} \gg 1$), Fig. 2 shows that the Fano resonance of the ring-coupled MZI is significantly sharper than the Lorentzian response of the single-bus ring. For example, when $\kappa_{\text{norm}} = 20$, the ring-coupled MZI is more than 16 times as sensitive as the single-bus ring. However, operating ring sensors in this overcoupled regime is suboptimal because in this regime neither of them has maximum sensitivity. Thus, while Fano resonances in a ring-coupled MZI may prove quite useful for applications where the loss is insignificant compared to coupling (such as in an optical switch), their benefits are considerably more modest in systems where the loss and coupling are comparable, such as sensors optimized for sensitivity purposes.

The 30.5% sensitivity enhancement predicted for the ring-coupled MZI differs significantly from the 8.2-fold enhancement reported in [13] for a ring coupled to a two-mode waveguide. Although the two systems are not exactly equivalent, we believe that a large fraction, if not most or all, of this discrepancy stems from the erroneous use in [13] of the fringe visibility as the metric to quantify sensitivity. The sensitivity defined in such terms depends only on the ratio of the intensities of the two signals being interfered, which means that it becomes infinite for vanishingly small signals, irrespective of the magnitude of the perturbation. Any sensor, including the ring-coupled MZI, can also have an arbitrarily large visibility-based "sensitivity." This definition is clearly not physically meaningful; also, it ignores the impact of noise on the minimum detectable perturbation. The sensitivity of sensors is customarily defined in terms of the *absolute* detected power change, as done here, for this reason. However, the configuration of [13] is sufficiently different from the ring-coupled MZI studied here that further investigations are needed to determine which of the two configurations has a higher true sensitivity after optimization.

The benefits of the ring-coupled MZI configuration (enhanced sensitivity and reduced circulating intensity) come at the cost of additional complexity, which may reduce its utility in practical systems. In particular, optimum sensitivity in the ring-coupled MZI requires that t_{ref} and Φ_{ref} be held constant in time, which means that the MZI must be stabilized in addition to the ring resonator. Thus, the thermal stabilization requirements of the ring-coupled MZI are more stringent than for a single-bus ring, a disadvantage that may outweigh the benefits of this device in practical applications.

5. Conclusions

In conclusion, we have demonstrated that an optimized ring-coupled MZI can achieve 30.5% greater sensitivity than an optimized single-bus ring resonator sensor. Unlike the single-bus sensor, this configuration achieves maximum sensitivity at critical coupling. While in the overcoupled regime the ring-coupled MZI offers a large sensitivity enhancement over the single-bus ring, the absolute sensitivity offered by the ring-coupled MZI is then much smaller than when the coupling of each of these sensors is optimized. The optimized ring-coupled MZI sensor also has 25% less power circulating in the ring resonator, which reduces the nonlinear Kerr effect. By decreasing the input power, the ring-coupled MZI can have the same sensitivity as an equivalent single-bus ring, but with 1.74 times less Kerr-induced phase drift. The increased sensitivity and reduced circulating power in this sensor come at the cost of reduced thermal stability, since the MZI must be stabilized in addition to the ring resonator.

This work was supported by Litton Systems, Inc., a wholly owned subsidiary of Northrop Grumman.

References

1. M. Sumetsky, "Optimization of optical ring resonator devices for sensing applications," Opt. Lett. **32**, 2577–2579 (2007).
2. Z. X. Xia, Y. Chen, and Z. P. Zhou, "Dual waveguide coupled microring resonator sensor based on intensity detection," IEEE J. Quantum Electron. **44**, 100–107 (2008).
3. C. Y. Chao and L. J. Guo, "Design and optimization of microring resonators in biochemical sensing applications," J. Lightwave Technol. **24**, 1395–1402 (2006).

4. A. Bananej and C. F. Li, "Controllable all-optical switch using an EDF-ring coupled M-Z interferometer," IEEE Photon. Technol. Lett. **16**, 2102–2104 (2004).
5. J. E. Heebner, V. Wong, A. Schweinsberg, R. W. Boyd, and D. J. Jackson, "Optical transmission characteristics of fiber ring resonators," IEEE J. Quantum Electron. **40**, 726–730 (2004).
6. J. E. Heebner, N. N. Lepeshkin, A. Schweinsberg, G. W. Wicks, R. W. Boyd, R. Grover, and P. T. Ho, "Enhanced linear and nonlinear optical phase response of AlGaAs microring resonators," Opt. Lett. **29**, 769–771 (2004).
7. J. E. Heebner and R. W. Boyd, "Enhanced all-optical switching by use of a nonlinear fiber ring resonator," Opt. Lett. **24**, 847–849 (1999).
8. Y. Lu, J. Q. Yao, X. F. Li, and P. Wang, "Tunable asymmetrical Fano resonance and bistability in a microcavity-resonator-coupled Mach-Zehnder interferometer," Opt. Lett. **30**, 3069–3071 (2005).
9. L. Y. Mario, S. Darmawan, and M. K. Chin, "Asymmetric Fano resonance and bistability for high extinction ratio, large modulation depth, and low power switching," Opt. Express **14**, 12770–12781 (2006).
10. P. P. Absil, J. V. Hryniewicz, B. E. Little, R. A. Wilson, L. G. Joneckis, and P. T. Ho, "Compact microring notch filters," IEEE Photon. Technol. Lett. **12**, 398–400 (2000).
11. L. J. Zhou and A. W. Poon, "Fano resonance-based electrically reconfigurable add-drop filters in silicon microring resonator-coupled Mach-Zehnder interferometers," Opt. Lett. **32**, 781–783 (2007).
12. S. Fan, "Sharp asymmetric line shapes in side-coupled waveguide-cavity systems," Appl. Phys. Lett. **80**, 908–910 (2002).
13. A. Ruege and R. Reano, "Multimode waveguide-cavity sensor based on fringe visibility detection," Opt. Express **17**, 4295–4305 (2009).
14. H. Lefèvre, *The Fiber-Optic Gyroscope* (Artech, 1993), Chap. 11.